Experimental 3-D SAR human target signature analysis

Brigitte Chan*[a], Pascale Sévigny[a], David D. J. DiFilippo[a]
[a]Defence R&D Canada, 3701 Carling Avenue, Ottawa, ON, Canada, K1A 0Z4

ABSTRACT

Defence Research & Development Canada has been investigating 3-D through wall synthetic aperture radar (SAR) imaging from an experimental L-band through-wall SAR prototype. Tools and algorithms for 3-D visualization are being developed to exploit the resulting imagery. In this paper, a comprehensive study of the characteristics of human target signatures in free space and behind two different wall structures is presented using 3-D SAR data. The aim of this investigation is to gain a better appreciation of the signatures of targets when placed behind different wall materials. An analysis of the human target signature in different poses is provided. There was very close agreement between the measured physical dimensions of the targets and those obtained from the strong returns in the SAR imagery. Viewing of the SAR data as 2-D slices provides a qualitative means of discriminating between different target signatures. A more useful approach to discrimination is to quantify these differences. The next phase of this investigation will look at different quantitative features as potential discriminants.

Keywords: through-wall, human target signature, L-band, SAR, detection, 3-D SAR

1. INTRODUCTION

The analysis of through-wall radar imagery is an emerging research area. Research has led to commercial products where devices are stationary during scanning [1 - 7]. Researchers continue to investigate through-wall radar technology using different systems and imaging techniques, for example, [8 - 12]. The capability to capture high-resolution 3-D radar imagery while moving at stand-off distances is not prominent in the literature. Development of a prototype 3-D through-wall synthetic aperture radar (SAR) system with this capability is currently underway [13]. The intent is to map out building wall layouts and to detect targets of interest behind walls such as humans, arms caches, and furniture. This situational awareness capability can be invaluable to the military working in an urban environment. The experimental SAR radar testbed operates in the L-band. The side-looking radar is truck-mounted with data collected as the vehicle is driven past the front of a building of interest. The system operates over a 1.86 GHz bandwidth between 0.85 and 2.71 GHz. It has two transmit and eight receive antennas [14]. The radar system is shown in Figure 1. It is complemented by a light detection and ranging system (LIDAR) and a positioning system, both truck-mounted as well, as seen in this figure. The LIDAR provides high resolution images of the exterior of a building. It adds another layer of information to help with the interpretation of the SAR data. The positioning system is used for motion compensation as well as to provide an accurate point of reference.

The SAR and LIDAR data are collected while the truck moves along the SAR path parallel to the building of interest. It is typically located approximately 10 meters from the front wall if the road structure allows. The azimuth direction is parallel to the SAR path while the range direction is perpendicular to it. Offline, following acquisition, the raw SAR data are pre-processed for proper formatting and motion compensation, pulse-compressed in range, and then a backprojection algorithm is applied to form the SAR image [15]. In this paper, the characteristics of free-space and through-wall target signatures using 3-D SAR data from this system are examined. An analysis of the human target signature in different poses is provided. Targets used in this investigation include a human in a standing position, a human standing with arms stretched out, a human kneeling, a human holding an AK47 in a vertical position, a human holding an AK47 in an angled position, and a human sitting in a chair, all at approximately 8-12m in range with reference to the truck-mounted radar system at closest approach. Photographs of the target positions are presented in Figure 2.

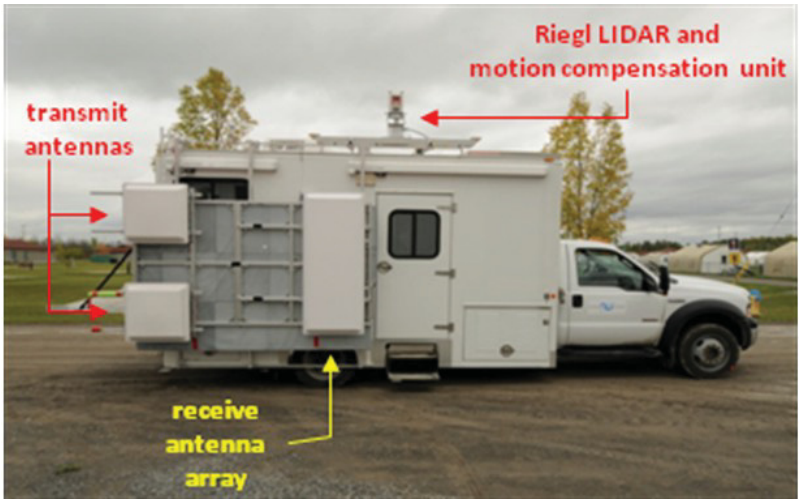

Figure 1. 3-D through-wall SAR system.

Figure 2. Photographs of the targets: (a) human standing arms down; (b) human standing arms stretched; (c) human kneeling; (d) human standing with AK47 in angled position; (e) human standing with AK47 in vertical position; (f) human sitting in chair.

A short description of the SAR data viewing platform to manually detect humans is provided in Section 2.0. In Section 3.0, free space signatures of the human in various poses are described. In Section 4.0, signatures of the human standing behind two different wall structures are described. In Section 5.0, conclusions and future research are presented.

2. VIEWING OF THE SAR DATA

To manually detect targets of interest, the 3-D SAR data are typically displayed in three 2-D slices that intersect at a pixel of interest (POI): one slice displays range vs. azimuth (top view), another slice displays elevation vs. azimuth (front view), and the last slice displays elevation vs. range (side view). An example is provided in Figure 3 where the white lines show the locations of the slices which intersect at the POI. Along the azimuth axis, values are displayed in reverse to emulate the SAR path taken by the vehicle during data collection. Along the elevation axis, the value of 0.0m is at ground/floor level. Values below ground/floor level appearing in the image represent the bottom part of the "curvature" created as a result of the point spread function. Viewing 2-D slices at different POIs provides a mechanism to manually detect the locations of targets of interest. When the POI is on-target at the highest intensity value of that target, the POI at that value becomes the pixel at maximum intensity (PMI). By convention, the radar path is always at the bottom for the top view images (truck going from right to left). Front view images are displayed as seen from the radar (truck going from right to left). Side view images are displayed with the radar to the left. The data were normalized to ensure scaling remained the same for all images.

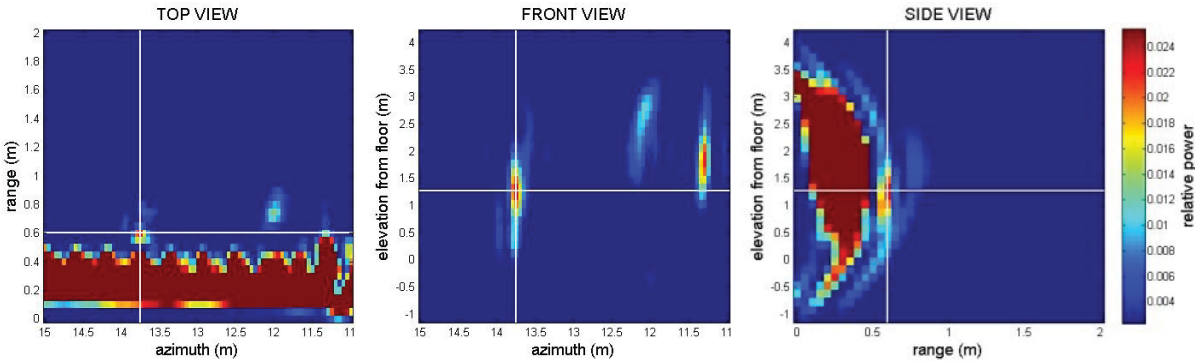

Figure 3. Through-wall SAR data as 2-D slice representations intersecting at a point of interest (POI) where a human target is located behind a wall.

3. HUMAN TARGET SIGNATURES IN FREE SPACE

All targets were manually detected and the corresponding PMIs were identified. The signature of a human target in free-space is examined for different body positions. The positions include a human standing with arms at his side, a human standing with both arms stretched parallel to the ground, a human kneeling, a human holding an AK47 in a vertical position, a human holding an AK47 in an angled position, an empty chair, and a human sitting in a chair.

According to simulation studies of the signatures of the human body in free space conducted by the United States Army Research Laboratory [16], the main contribution to the radar return comes from the human torso. They conclude that arms and shoulders contribute to bright spots on the sides of the torso, that the legs contribute to a "late-time" return caused by the effect of double bouncing of the incident wave from one leg to the other before transmission to the receive antenna, and that there is significant backscatter appearing to come from behind the main return corresponding to the torso. Here, a comparison of the results of those simulations using 3-D SAR images of human targets in free space is conducted, with the added advantage of examining how the backscatter varies with elevation.

Twelve different subjects were examined for the human standing position, standing between 8m and 12m away from the radar in range and standing on gravel or asphalt. Subjects varied in height and size. Resolution is less than 15cm in range and azimuth and 5.2 degrees in elevation. The strongest return can be seen at PMI elevations between the feet and the hips (less than 1m), which is different than the expected strongest return reported in [16]. Given the elevation resolution of 1m at a distance of 10m from the radar, this suggests that the strongest return does not come from the human torso but rather from the interaction between the ground and legs, where a corner is formed.

A typical 3-D SAR image is displayed as progressive top view 2-D slices at varying elevation in Figure 4 for elevations between -0.25m and 1.25m, at steps of 50cm (half the elevation resolution at a distance of 10m from the radar). The black lines show the locations of the slices which intersect at the PMI, with the value of 0.0m in elevation signifying at ground level. The strongest returns (0dB) occur at elevations from 0.25m to 1.25m. This 1m variation in elevation could be expected considering the elevation resolution. Two secondary returns (approximately -10dB) are present. They can be attributed to point scatterers located where the shoulder features are expected and where the double bounce from the leg features are expected, as was reported in the simulations of the human signature in [16]. The front and side view 2-D slices at the PMI of the 3-D SAR data in Figure 5 makes it possible to view the difference in elevation between the different features. In the front view image, the interaction between the ground and each foot is evident with a slight separation in azimuth between each feature. The strongest return is seen at knee level but a very strong return is also visible at the height corresponding to the human torso. In the side view image, the difference in range between the ground and leg interaction and the late return caused by the double bounce of the legs is discernible.

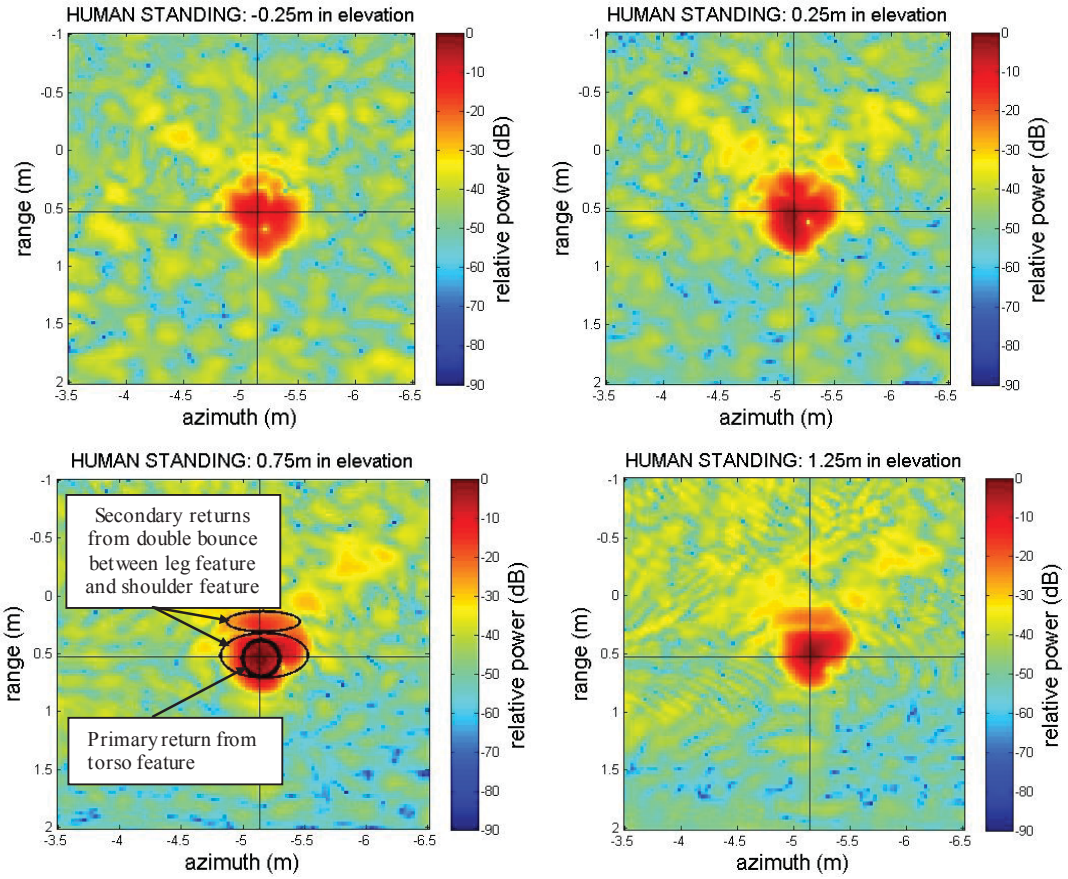

Figure 4. Top view 2-D slices of human target in standing position at varying elevations.

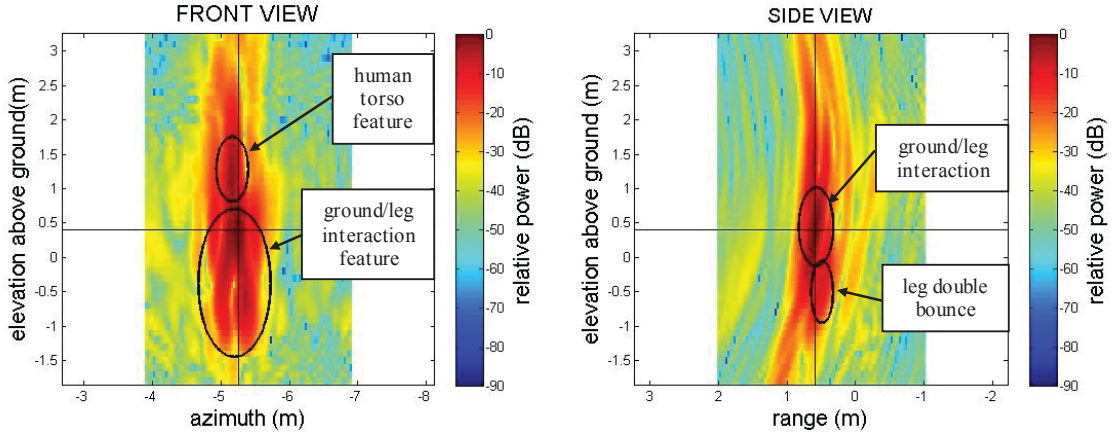

Figure 5. Front view and side view 2-D slice of human target in standing position.

The top, front, and side view 2-D slices at the PMI of the 3-D SAR data of the human target in four different positions is shown in Figure 6. Positions include: standing with arms stretched, kneeling, holding AK47 at an angle, holding AK47 vertically. The top, front, and side view 2-D slices at the PMI of the 3-D SAR data of an empty chair and a human sitting in a chair are shown in Figure 7.

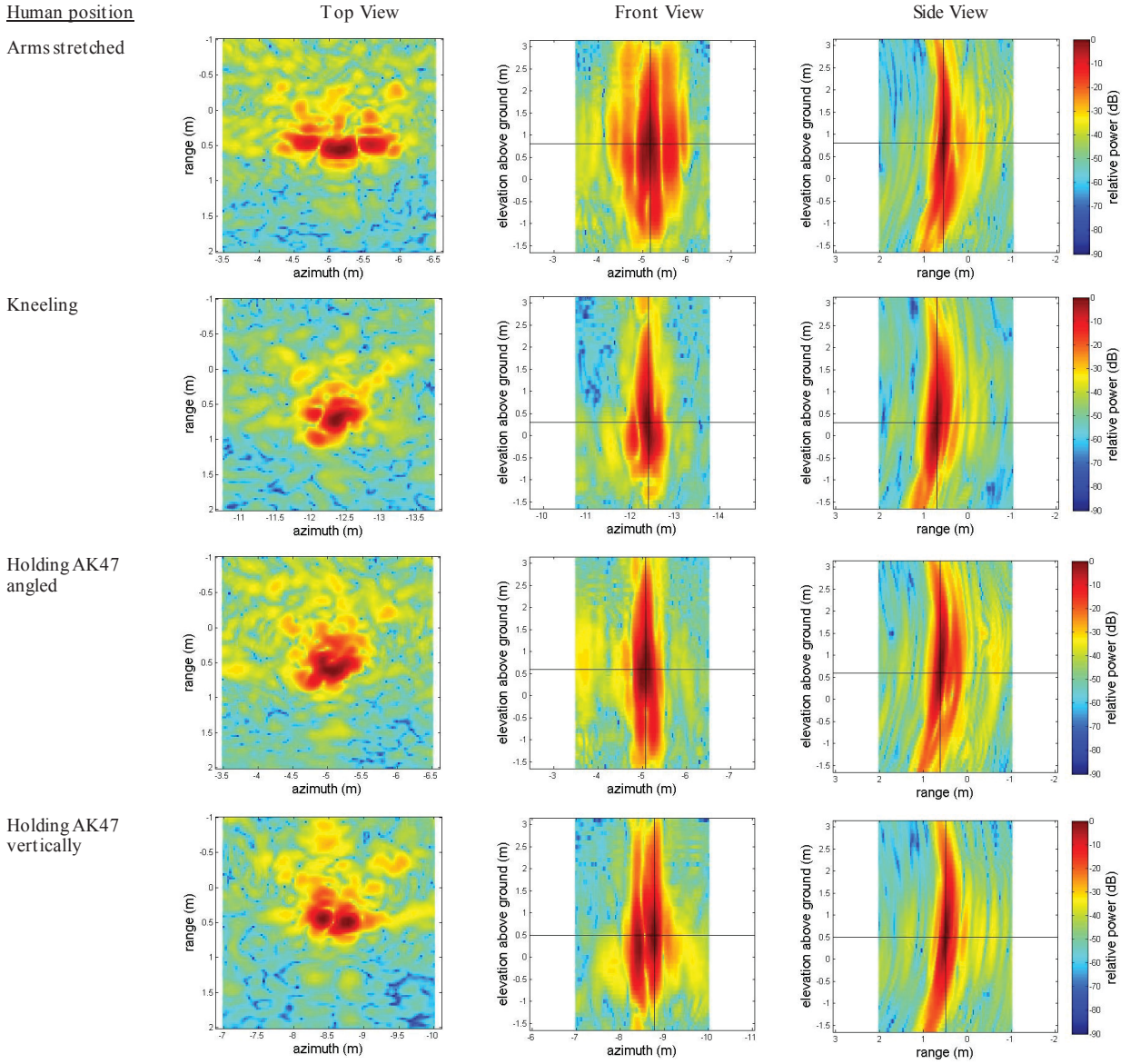

Figure 6. Top, front, and side view 2-D slices of human target in different positions.

In the human standing with arms stretched images, the torso and the extended arms of the human are readily discernible in the top view. The extent of the arm features in azimuth is evident. The strong returns are caused by the corner created between the arms and the body. Significant returns are once again seen behind the main torso and at the ground level where the ground and legs form a corner.

In the human kneeling top view image, the forward knee feature appears closer in range on the left side while the back foot feature appears further in range and weaker on the right side. The difference in signature between the human standing and human kneeling is most evident in the front view image, where the energy is more concentrated near the ground level, giving the appearance of a bulb. Furthermore, the ground/foot separation feature seen in the human standing case is not present in the human kneeling signature.

In the top view image of the human holding an AK47 in an angled position across its chest, the signature is very similar to the human kneeling one. The only discernible difference is the shape of the strongest return; more circular in the human kneeling case versus more of an arc in the human holding an AK47 in an angled position case. In the side view image, a late return that is brighter and extends further in range than the human standing case is visible. This is due to the multiple bounces between the AK47 and the human body, where many corners are formed. In the human holding an AK47 vertically top and front view images, two distinct strong returns are visible side by side. One represents the human standing return while the other represents the AK47 return. Both are of the same intensity.

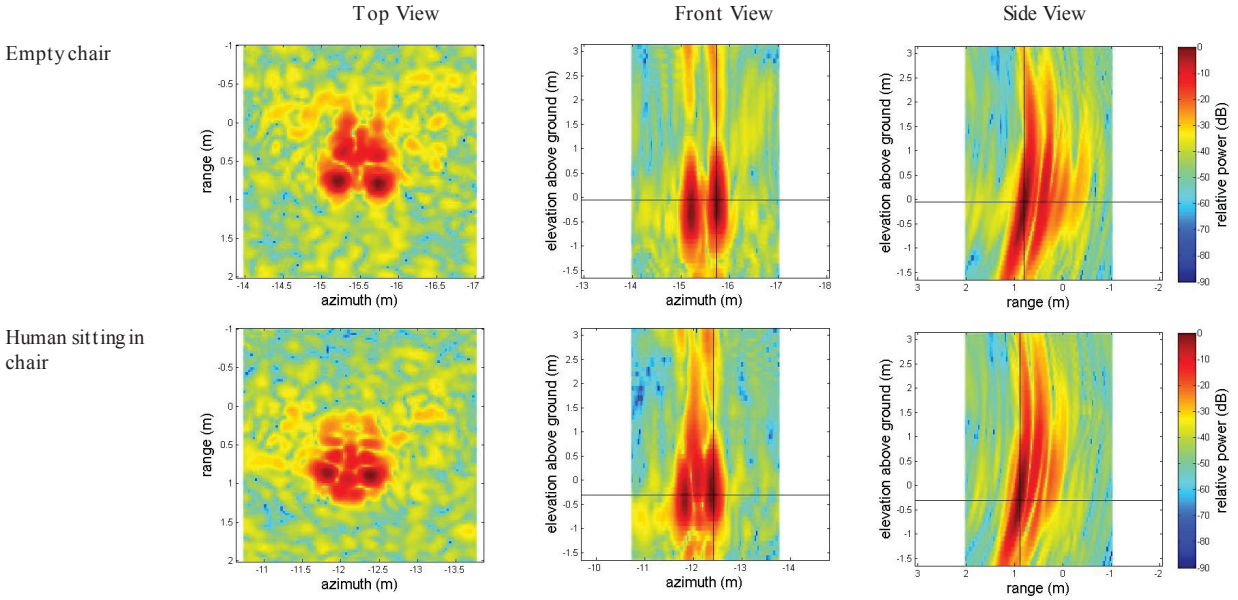

Figure 7. Top, front, and side view 2-D slices of an empty chair and a human target sitting in a chair.

The signature of a chair in free-space is presented in Figure 7. The chair is composed of three materials: metal, cloth, and plastic. The chair legs which support the armrest and back, as well as the cushion support brackets underneath the chair, are metallic. The armrests are hard plastic. The seat cushion and chair back consist of a cloth material covering foam and corkboard. Only the metallic pieces are expected to have strong SAR returns. Five strong point returns are identifiable in the SAR images of the empty chair. Four of the strong returns correspond to each of the four metal legs of the chair, as expected. The PMI elevation coordinates for each chair leg correspond to the corners created between the ground and each leg. The fifth return is the strongest and is centrally located between the right and left legs in the azimuth direction and is positioned at the same range as the back legs. When looking at the metal frame supporting the cushion, it becomes clear that a wide angled metallic corner is formed at the junction between each half of the bracket. This corner is what is creating the fifth large return in the SAR data. It is approximately 20cm further in range than its physical location because the microwave signal bounces between the two sides of the bracket, resulting in a delay before returning to the radar. In the front view of the empty chair image, the two front chair leg returns are visible. In the side view of the image, the strongest return of the front legs is visible with the back legs and late return from the metallic bracket visible further in range.

In the top view image of the human sitting in a chair, a strong return where the ground and the human legs create a corner is visible with the front chair leg features being brightest. Compared to the empty chair signature, the features of the back legs and the metallic brackets are weaker. This is due to the reduction in illumination from the radar signal as the signal now has to pass through and around the human to reach the back legs and brackets. The weaker returns further in range are also seen in the side view image. In the front view image, the strong return from the human is evident in between the two front chair leg returns.

In free space, the human standing signature can visually be differentiated from the human in different positions when looking at 2-D slices in the top, side, and front views. Having gained a better appreciation of the signatures of human

targets in free space, the next step is to investigate what happens to the signature when the human is placed behind different wall materials.

4. HUMAN TARGET SIGNATURES BEHIND WALLS

The signature of the human target behind two different wall structures is examined in this section. All targets were manually detected and the corresponding PMIs were identified.

The first wall structure is a fairly transparent one constructed of drywall made of wood studs, gypsum, insulating material, and vinyl coating on the exterior. A LIDAR image of the inside of the building with the location of the human target is shown in Figure 8. The human target is positioned 1.6m behind the wall in between two windows. For this scenario, the signature of a human target is examined for four different body positions. The positions include a human standing, a human kneeling, a human holding an AK47 in an angled position, and a human holding an AK47 in a vertical position. The top, front, and side view 2-D slices at the PMI of the 3-D SAR data of the human target in these four different positions is shown in Figure 9. The location of the target is indicated by a black circle in the top view images. In each case, part of the wall signature appears at a range of -6m. Even behind a relatively transparent wall such as drywall, there is a significant increase in the amount of clutter and multipath.

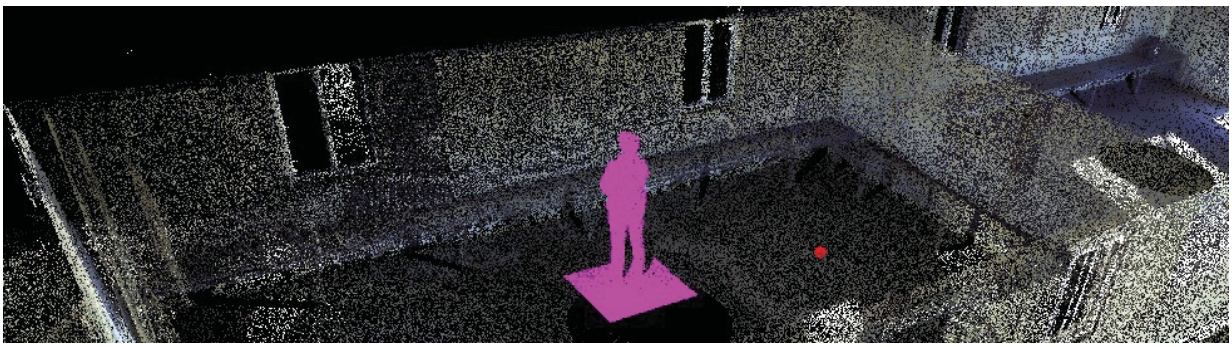

Figure 8. LIDAR imagery of a human standing inside a building constructed of drywall made of wood stud, gypsum, insulating material, and vinyl coating.

In the human standing images, three bright spots at the location of the target at the same range are visible in the top view where only one bright spot is expected. They are all circular in shape. The middle return is similar to the one seen in free space but appears out of focus. This is expected considering the different paths through the wall structure that the radar signal must travel to get to the target, such as through and around studs. The different features from the floor/leg interaction, shoulders, and double bounce from the leg that were visible in the free space case are not discernible. In the front view image, the strong return from the floor/leg interaction combined with the strong return from the torso seems to dominate the signature. A small separation between the ground and each foot that was seen with the human standing in free space signature is also visible here. In the side view image, it is difficult to differentiate the late return from the double bounce of the legs and the clutter. The two bright spots on each side of the main human signature could be ghosts, caused by multipath. This phenomenon is currently being investigated.

In the human kneeling top view image, two similarly strong returns are visible diagonally from each other. The right strong return is the target signature whereas the left strong return could be a ghost. The forward knee and back foot features of both returns are still visible, similarly to the free space human kneeling signature. In the front view image, there is considerably less energy in higher elevation for the kneeling target compared to the human standing behind the wall case. For the return that could be a ghost, the energy is spreads higher in elevation. In the side view image, it is difficult to differentiate the returns from the clutter.

In the top view image of the human holding an AK47 in an angled position across its chest, the signature is very different from the human kneeling one. It resembles more of the human standing signature behind the wall. Three bright spots are visible at slightly different ranges. In the front view image, the two side returns are visible at the same elevation. In the side view image, the late return due to the multiple bounces between the AK47 and the human body is present. In the

human holding an AK47 vertically top view image, there are several strong returns visible. It is difficult to distinguish between the different features. Several ghosts could be overlapping with the main returns, giving the appearance of a highly cluttered environment. Clutter also seems to overwhelm the front view image.

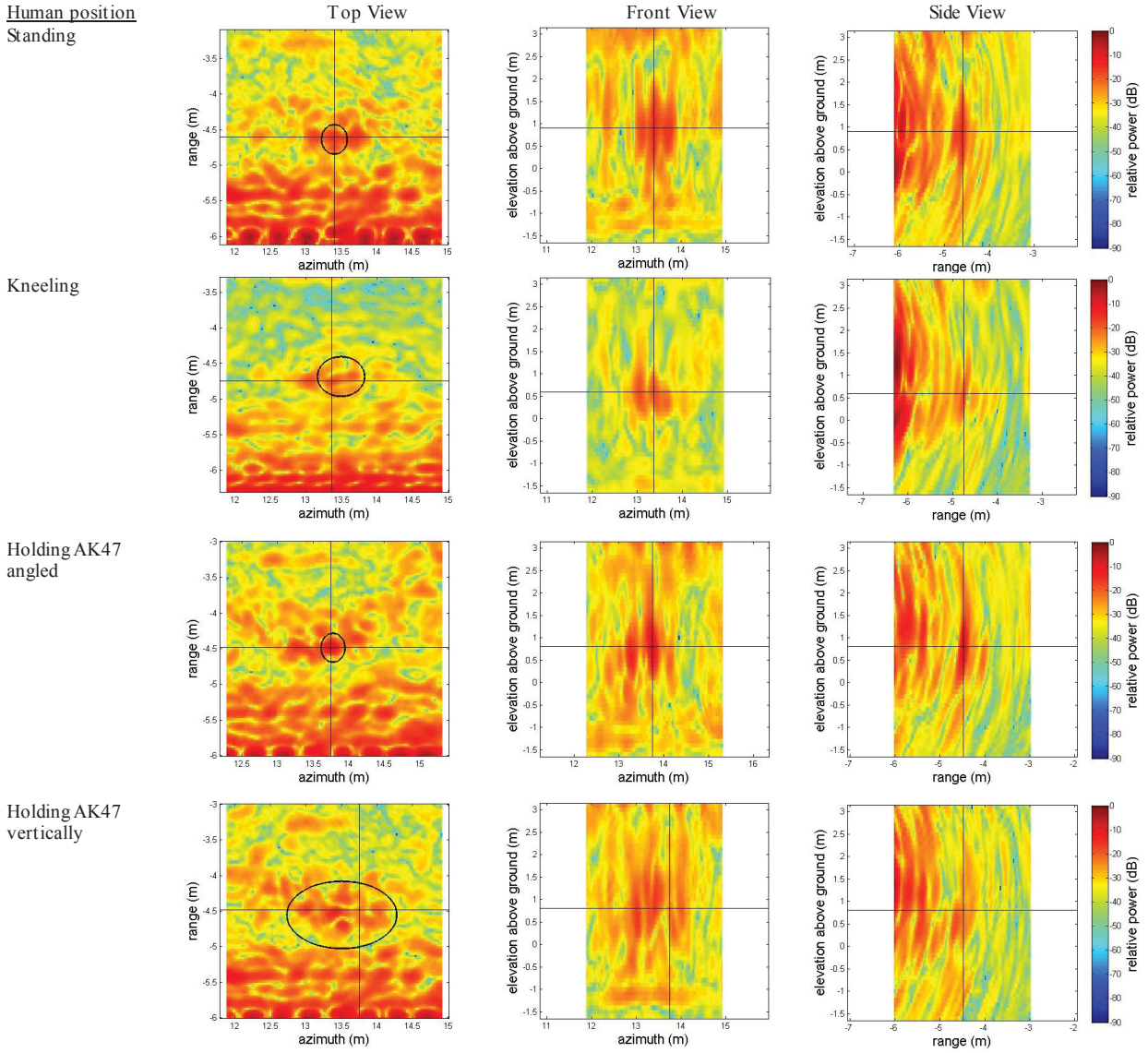

Figure 9. Top, front, and side view 2-D slices of human target in different positions behind a wall constructed of drywall made of wood stud, gypsum, insulating material, and vinyl coating.

The second wall structure is made of cinder blocks and is a more challenging wall to penetrate with the radar. A LIDAR image of the inside of the building with the location of the human target is shown in Figure 10. The human target is positioned 1.6m behind the wall. The wall structure contains no window or door. For this scenario, the signature of a human target is examined for the human standing position only. The top, front, and side view 2-D slices at the PMI of the 3-D SAR data of the human target is shown in Figure 11. The location of the target is indicated by a black circle in the top view image. Part of the wall signature appears at a range of -0.5m. In the images, the high clutter environment behind a cinder block is evident. Even so, the human standing target can still be manually detected.

One bright spot at the location of the target is visible in the top view image. The strong return is circular and similar to the one seen behind a drywall structure, appearing out of focus. This is expected considering the different paths through the air gaps of the cinder blocks that the radar signal must travel to get to the target. Again, the different features from the floor/leg interaction, shoulders, and double bounce from the leg that were visible in the free space case are not discernible. Several other bright spots are visible in the image, some of which could be considered clutter and some could be ghosts. In the front view image, the strong return from the floor/leg interaction combined with the strong return from the torso seems to dominate the signature. The small separation between the ground and each foot that was seen with the human standing in free space signature is not visible here. In the side view image, the clutter overwhelms the image.

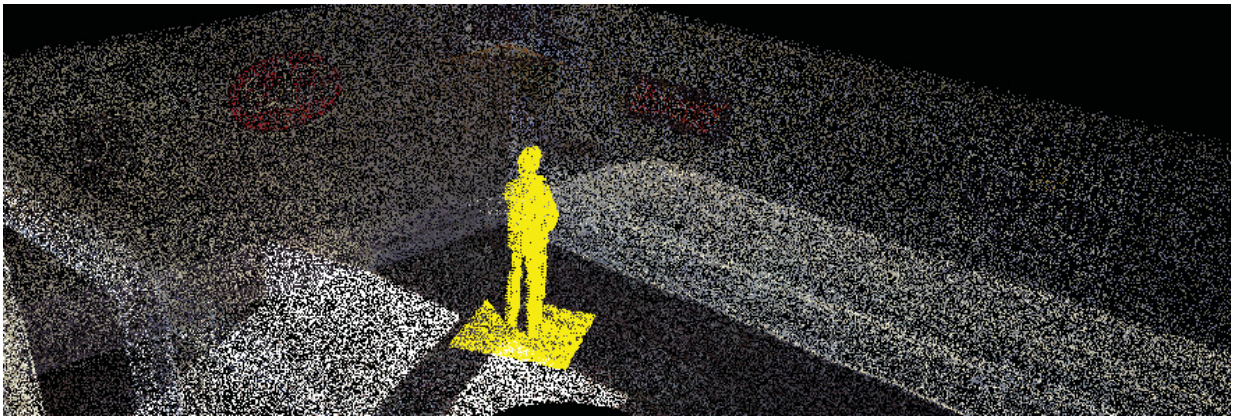

Figure 10. LIDAR imagery of a human standing inside a building constructed of cinder blocks.

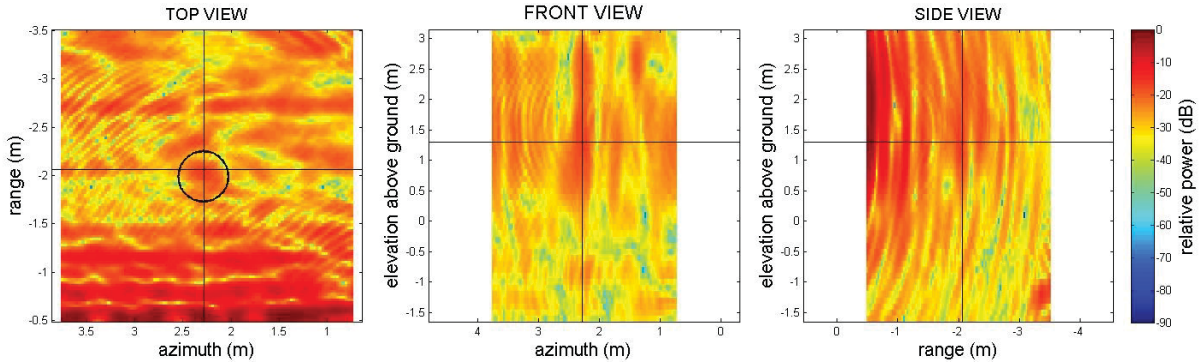

Figure 11. Top, front, and side view 2-D slices of human target in different positions behind a cinder block wall.

5. DISCUSSION AND CONCLUSIONS

Tools and algorithms for 3-D visualization are being developed for the analysis of signatures of human targets behind a wall and to develop an understanding of the clutter and multipath signals in a room of interest. In this report, a comprehensive study of the characteristics of free-space and through-wall target signatures were presented using 3-D SAR data. The aim of this investigation was to gain a better appreciation of the signatures of targets placed behind different wall materials which could help in identifying potential discriminants for classification of human targets. Radar signatures in 3-D SAR imagery were studied for the human target in different positions in free space and behind two different wall structures. There was very close agreement between simulations and the strong SAR image returns produced from the human standing target in free space. Most of the sources of the strong returns seen in the SAR images were explained, taking into consideration the location of the PMI, the measurements between different returns, and the location of the strong returns with respect to different physical features of each target, such as corners formed.

Viewing of the SAR data as 2-D slices provides a qualitative means of investigating the human target signature. A more useful approach to discrimination would be to quantify these differences. The next phase of this investigation is to look at different quantitative features as potential discriminants. Furthermore, a thorough understanding of the clutter and multipath present behind walls are required if the signature of the human target is to be extracted and discriminated from these noise sources. Eventually, efforts will be made to choose the most effective classifier for the discrimination of human targets from all others.

REFERENCES

[1] Prism 200: Through Wall Radar, Cambridge Consultants, June 11, 2014, http://www.cambridgeconsultants.com/projects/prism-200-through-wall-radar

[2] Xaver Products, Camero, June 11, 2014, http://www.camero-tech.com/products.php

[3] EMMDAR (Electro-Magnetic Motion detection And Ranging), L3 CyTerra, June 11, 2014, http://www.cyterra.com/products/emmdar.htm

[4] Range-R, L3 CyTerra, June 11, 2014, http://www.cyterra.com/products/ranger.htm

[5] ASTIR: Standoff Through-Wall Imaging Radar, Akela, June 11, 2014, http://www.akelainc.com/products/astir

[6] CPR-4, Cinside, June 11, 2014, http://cinside.se/e/products/cinside-cpr4

[7] O-PEN Radar, SRC, June 11, 2014, http://www.srcinc.com/what-we-do/radar-and-sensors/o-pen-radar.html

[8] Amin, M. G., [Through-the-wall RADAR imaging], CRC Press, Florida (2011).

[9] Ralston, T. S., Charvat, G. L., Peabody, J. E., "Real-time through-wall imaging using an ultrawideband multiple-input multiple-output (MIMO) phased array radar system," IEEE International Symposium on Phased Array Systems and Technology, 551-558 (2010).

[10] Chetty, K., Smith, G. E., Woodbridge, K., "Through-the-wall sensing of personnel using passive bistatic WiFi radar at standoff distances," IEEE Trans. On Geoscience and Remote Sensing, 50(4), 1218-1226 (2012).

[11] Riaz, M. M., Ghafoor, A., "Principle component analysis and fuzzy logic based through wall image enhancement," Progress in electromagnetic Research, 127, 461-478 (2012)

[12] Shirodkar, S., Barua, P., D, Anuradha, Kuloor, R., "Heart-beat detection and ranging through a wall using ultra wide band radar," IEEE International Conference on Communications and Signal Processing, 579-583 (2011).

[13] Sévigny, P., DiFilippo, D., Laneve, T., Chan, B., Fournier, J., Roy, S., Ricard, B., Maheux, J., "Concept of operation and preliminary experimental results of the DRDC through-wall SAR system," Proceedings of SPIE 7669, 766907, doi: 10.117/12.849709 (2010).

[14] Raut, S., Petosa, A., "A compact printed bowtie antenna for ultra-wideband applications," Proceedings of European Microwave Conference, 081-084 (2009).

[15] Soumekh, M., [Synthetic aperture radar signal processing], John Wiley and Sons, 1999.

[16] Dogaru, T., Nguyen, L., Le, C., "Computer models of the human body signature for sensing through the wall radar applications," Army Research Lab ARL-TR-4290, (2007).